

The size and polydispersity of silica nanoparticles under simulated hot spring conditions

D. J. TOBLER^{1,*}, L. G. BENNING¹ AND J. KNAPP²

¹ Earth and Biosphere Institute, School of Earth and Environment, University of Leeds, Leeds, LS2 9JT, UK

² Institute of Integrative and Comparative Biology, Faculty of Biological Science, University of Leeds, Leeds, LS2 9JT, UK

ABSTRACT

The nucleation and growth of silica nanoparticles in supersaturated geothermal waters was simulated using a flow-through geothermal simulator system. The effect of silica concentration ($[\text{SiO}_2]$), ionic strength (IS), temperature (T) and organic additives on the size and polydispersity of the forming silica nanoparticles was quantified. A decrease in temperature (58 to 33°C) and the addition of glucose restricted particle growth to sizes <20 nm, while varying $[\text{SiO}_2]$ or IS did not affect the size (30–35 nm) and polydispersity (± 9 nm) observed at 58°C. Conversely, the addition of xanthan gum induced the development of thin films that enhanced silica aggregation.

KEYWORDS: silica nanoparticles, size distribution, hot springs.

Introduction

THE precipitation of silica in active geothermal systems is a well-known process leading to the silicification of microorganisms and the formation of silica sinters. Several studies have considered the interactions between microorganisms and inorganically nucleating silica particles in both field and experimental studies (e.g. Mountain *et al.*, 2003; Benning and Mountain, 2004 and references therein), or have investigated the mechanisms and kinetics of silica nanoparticle formation in inorganic solutions (e.g. Iler, 1979; Rimstidt and Barnes, 1980; Icopini *et al.*, 2005). However, in all laboratory studies, silica polymerization was induced by a pH change, yet in natural systems (e.g. geothermal pools) silica polymerization and nanoparticle formation are a result of rapid cooling of a supersaturated near neutral fluid.

Here we present data from a study where silica polymerization and nanoparticle formation was followed using a flow-through geothermal simulator system where polymerization was induced

by rapid cooling. Changes in $[\text{SiO}_2]$, IS, T or organic additives (i.e. glucose, xanthan gum, representing microbial cell wall functional groups) and their effect on silica polymerization were quantified via the time dependent depletion in monomeric silica and the changes in size and polydispersity of growing silica nanoparticles.

Methods

A high-temperature flow-through geothermal simulator system (Fig. 1) was used to equilibrate a supersaturated silica solution ($[\text{SiO}_2] = 640$ or 960 ppm, IS = 0.02 or 0.11, pH = neutral) in a high-temperature oven ($\sim 230^\circ\text{C}$) in order to fully de-polymerize it prior to the experiments (2.5 h residence time). After passing through a back-pressure regulator, BPR, the solutions were led via Teflon tubing into a Teflon tray inside an incubator (at 33 or 58°C). This cooling simulated the conditions of a supersaturated deep fluid being discharged in a hot spring (i.e. induction of silica polymerization, but constant re-supply of fresh solution). Organics were added to the tray via an additional pump, which measured out exact concentrations of either glucose or xanthan gum (Table 1).

* E-mail: tobler@see.leeds.ac.uk

DOI: 10.1180/minmag.2008.072.1.287

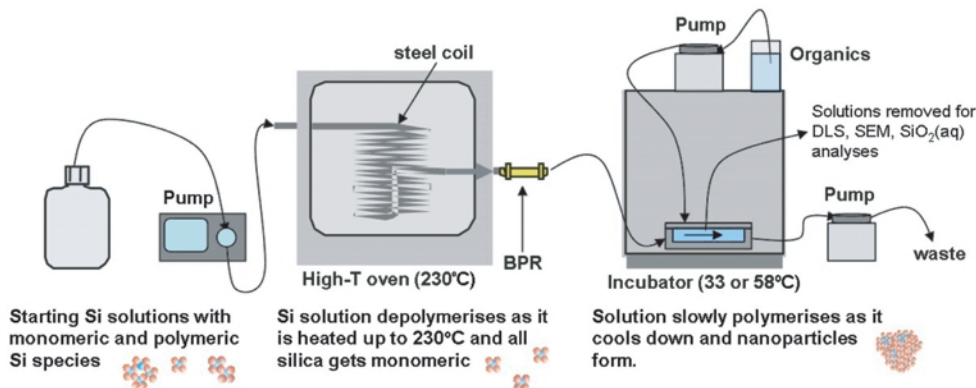


Fig. 1. Sketch of the simulated hot spring system (modified after Benning and Mountain, 2004).

Samples were removed from the middle of the tray (solutions polymerized for ~ 1 h) and the monomeric silica, $[\text{SiO}_{2(\text{aq})}]$, and total silica concentration, $[\text{SiO}_2]$, (molybdate yellow method after Greenberg *et al.*, 1985) were monitored over 31 h. Changes in silica particle size distribution and polydispersity were derived from high-resolution scanning electron microscopic (SEM) images or via direct solution analysis using standard dynamic light scattering (DLS, Malvern Nanosizer).

Results and discussion

Monomeric SiO_2 variations

In most inorganic experiments during the first 9–11 h, a 10–15% increase in $[\text{SiO}_{2(\text{aq})}]$ was observed which correlated with the time needed to establish a steady state within the tray. At

equilibrium, the $[\text{SiO}_{2(\text{aq})}]$ values were about twice as large (between 325 and 425 ppm) as the silica solubility calculated for the tested conditions (e.g. 136 ppm for 33°C and 209 ppm for 58°C; Gunnarsson and Arnórsson, 2000). This confirmed that the constant re-supply of new solution guaranteed a continual polymerization reaction.

Overall, in terms of $[\text{SiO}_{2(\text{aq})}]$, few differences were observed as a consequence of changing T , $[\text{SiO}_2]$, IS or organics, yet the trends followed those dictated by the degree of silica saturation (i.e. larger IS, larger $[\text{SiO}_2]$ and lower T all decrease silica solubility; e.g. Iler, 1979). For the experiments with organics it is worth noting that large fluctuations in $[\text{SiO}_{2(\text{aq})}]$ were observed (specifically in the case of glucose) making it difficult to ascertain their impact on the polymerization process.

TABLE 1. Experimental conditions, mean diameter (d_{mean}) and polydispersity (st.dev.) measured after 7 and 31 h (DLS values are marked with *). GL: 300 ppm glucose; XG: 50 ppm xanthan gum.

| Exp. # | $[\text{SiO}_2]$ (ppm) | IS | T (°C) | $d_{\text{mean}} \pm \text{st.dev. (nm)}$ $t = 7 \text{ h}$ | $d_{\text{mean}} \pm \text{st.dev. (nm)}$ $t = 31 \text{ h}$ |
|-----------------------|------------------------|------|----------|--|---|
| Inorganic experiments | | | | | |
| E1 | 640 | 0.02 | 58 | 29±4 24±5* | 36±9 37±10* |
| E2 | 640 | 0.11 | 58 | 26±3 | — |
| E3 | 960 | 0.02 | 58 | 25±4 | 19±5 |
| E4 | 640 | 0.02 | 33 | 14±2 | 10±1.5 |
| Organic experiments | | | | | |
| E5 | Identical to E1 + GL | | | 15±3 | 15±4 |
| E6 | Identical to E1 + XG | | | — | — |

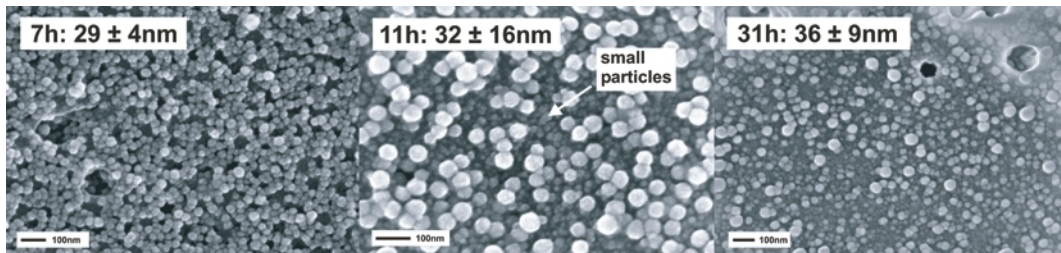


FIG. 2. SEM micrographs of silica nanoparticles formed after 7, 11 and 31 h (E1 experiment) with the mean diameter and polydispersity for each time step.

Size analysis

The size distributions obtained from most inorganic experiments at 58°C showed an increase in mean particle diameter over the first 9 h (from ~18 to 32 nm) followed by stabilization at a constant value (Figs 2 and 3, Table 1, both SEM and DLS data). Similarly, the polydispersity of the particles progressively increased until $t = 9$ h (± 5 nm) but then significantly increased over the following 2 h (from 5 to 16 nm) due to the occurrence of two size populations (see Fig. 2, 11 h). As the system stabilized (>11 h), the polydispersity equilibrated at ± 9 nm and this suggests that new particles nucleated continuously while older particles were still growing. However, once a steady state was established the mean

particle diameter and polydispersity were constant and no additional growth was observed, thus continuous nucleation and growth of new, smaller particles was favoured.

The biggest effects on size distribution and polydispersity were observed with decreasing temperature and the amount of added glucose (E5 and E5, Table 1 and Fig. 3). At 33°C an increased nucleation rate but little growth was observed. Once nucleated the particles did not grow larger than 14 ± 2 nm, and due to the continual re-supply of fresh solution the steady formation of new, smaller particle formation was favoured. Glucose (E5) followed the same trend with particle growth being restricted to sizes below 15 ± 4 nm. Conversely, in the presence of

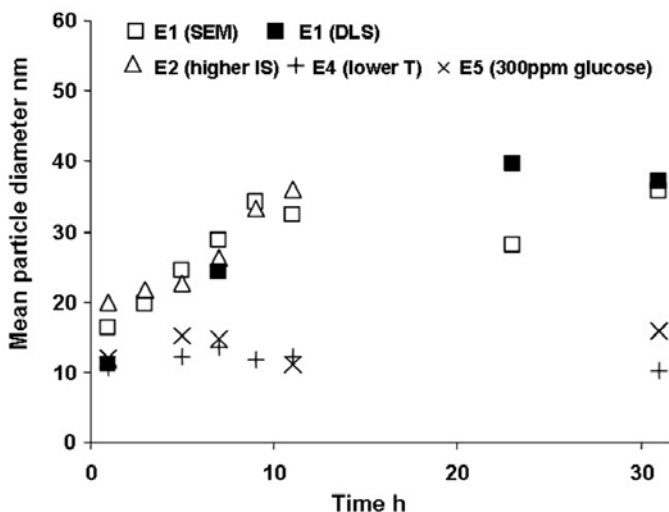


FIG. 3. Variation in mean diameter of silica nanoparticles with incubation time as a function of varying parameters, i.e. T , IS, organics (evaluated from SEM and DLS; polydispersity are not shown for clarity). For SEM ~100 particles were measured for each data point.

xanthan gum (E6) no particles could be detected in suspension but a thin film developed in the tray. This film enhanced the aggregation of silica to large clusters, confirming previous observations (Benning and Mountain, 2004).

All these findings compared well with recent field-based *in situ* silicification experiments carried out in Icelandic hot springs (Tobler, 2008) where the size range of silica nanoparticles within freshly deposited sinters were significantly larger at higher temperatures, although their sizes were less affected by silica concentration and ionic strength.

Conclusions

A successful hydrothermal experimental approach that simulates processes observed in natural geothermal springs has been developed. In all experiments, silica was highly supersaturated and silica polymerization and silica nanoparticle formation was initiated by a temperature-drop approach (i.e. simulates geothermal water being discharged at the surface). The results showed that:

(1) An increase in ionic strength or silica concentration had only minor effects on size and polydispersity of silica nanoparticles, while a lower temperature substantially influenced the size range of the forming particles (i.e. smaller particle sizes at lower temperatures).

(2) In the presence of glucose (a model simple organic compound) particle growth was restricted. On the contrary, xanthan gum (a complex polysaccharide) induced the development of thin silica-rich films at the air-water interface and only promoted silica aggregation; this confirmed that exopolymeric substances play a role in and aid the silicification and preservation of biofilms as previously observed in geothermal hot springs (e.g. Mountain *et al.*, 2003; Tobler, 2008).

Acknowledgements

Funding from the Leeds Earth and Biosphere Institute (DT) and University of Leeds (LGB and JK) is acknowledged.

References

- Benning, L.G. and Mountain, B.M. (2004) The silicification of microorganisms: a comparison between *in situ* experiments in the field and laboratory. Pp. 3–10 in: *Water-Rock Interaction* (R.B. Wanty and R.R. Seal, editors). Taylor and Francis Group, London. Carroll, S., Mroczek, E., Alai, M. and Ebert, M. (1998) Amorphous silica precipitation (60 to 120°C): Comparison of laboratory and field rates. *Geochimica et Cosmochimica Acta*, **62**, 1379–1396.
- Greenberg, A.E., Trussell, R.R. and Clesceri, L. (1985) *Standard Methods for the Examination of Water and Wastewater*. American Public Health Association, New York, 209 pp.
- Gunnarsson, I. and Arnórsson, S. (2000) Amorphous silica solubility and the thermodynamic properties of H₄SiO₄ in the range of 0 to 350°C at P_{sat}. *Geochimica et Cosmochimica Acta*, **64**, 2295–2307.
- Icopini, G.A., Brantley, S.L. and Heaney, P.J. (2005) Kinetics of silica oligomerization and nanocolloid formation as a function of pH and ionic strength at 25°C. *Geochimica et Cosmochimica Acta*, **69**, 293–303.
- Iler, R.K. (1979) *The Chemistry of Silica*. John Wiley, New York.
- Mountain, B.W., Benning, L.G. and Boerema, J. (2003) Experimental studies on New Zealand hot spring sinters: rates of growth and textural development. *Canadian Journal of Earth Sciences*, **40**, 1643–1667.
- Rimstidt, J.D. and Barnes, H.L. (1980) The kinetics of silica-water reactions. *Geochimica et Cosmochimica Acta*, **44**, 1683–1699.
- Tobler, D.J. (2008) *Molecular pathways of silica nanoparticle formation and biosilicification*. PhD thesis, University of Leeds, UK.